

01 Jan 1990

## Coatings And Surface Modification By Methane Plasma Polymerization

Chung-Peng -P Ho

H. Yasuda

Missouri University of Science and Technology, yasudah@mizzou.edu

Follow this and additional works at: [https://scholarsmine.mst.edu/chem\\_facwork](https://scholarsmine.mst.edu/chem_facwork)

 Part of the [Chemistry Commons](#)

---

### Recommended Citation

C. -. Ho and H. Yasuda, "Coatings And Surface Modification By Methane Plasma Polymerization," *Journal of Applied Polymer Science*, vol. 39, no. 7, pp. 1541 - 1552, Wiley, Jan 1990.

The definitive version is available at <https://doi.org/10.1002/app.1990.070390712>

This Article - Journal is brought to you for free and open access by Scholars' Mine. It has been accepted for inclusion in Chemistry Faculty Research & Creative Works by an authorized administrator of Scholars' Mine. This work is protected by U. S. Copyright Law. Unauthorized use including reproduction for redistribution requires the permission of the copyright holder. For more information, please contact [scholarsmine@mst.edu](mailto:scholarsmine@mst.edu).

# Coatings and Surface Modification by Methane Plasma Polymerization

CHUNG-PENG HO and H. YASUDA, *Institute for Thin Film Processing Science, Material Research Center, University of Missouri-Rolla, Rolla, Missouri 65401*

## Synopsis

Polymers formed from plasma-polymerized methane were employed to modify the surface properties of silicone rubber membrane. Polymers were evaluated based on the energy input parameter  $W/FM$ , where  $W$  is the discharge power,  $F$  is the monomer flow rate, and  $M$  is the molecular weight of the monomer. Dealing with the characteristics of plasma polymerization and the deposited polymer film, the effect of pumping rate on deposition rate and the coating thickness, surface energy, and gas permeabilities of methane-plasma-polymer-coated silicone rubber membrane were investigated in three plasma regions. Because more reactive species are expelled at high pumping rates, the monomer-deficient region is reached at lower  $W/FM$  in the high pumping rate system than that in the low pumping rate system. The composite parameter  $W/FM$  had a strong influence on coating thickness, gas permeability, surface energy, and the polar component of the surface energy but little effect on its dispersion component. Examination of gas permeabilities indicated that coating thickness was another important controlling factor on the properties of plasma polymer.

## INTRODUCTION

Since 1953, when Silastic S-9711, the first silicone rubber made for medical investigation, was developed by Dow Corning Corp., much research has taken place on the medical application of silicones. Owing to its special properties, such as high gas permeability, insignificant toxicity, biological inertness, superior tissue compatibility, and blood compatibility, silicone rubber has been used in many kinds of prosthetic applications. Nevertheless, the intrinsic tackiness and hydrophobicity of the surfaces of silicone rubber materials are disadvantages in some specific biomedical applications, and they are difficult to alter by common chemical methods without losing the favorable properties of the material.

The unique technique of glow discharge polymerization is capable of producing crosslinked, pin-hole free, thin films of organic polymer. It can also be used to widely vary the properties of the substrate surface without changing its bulk properties when a plasma polymer film is deposited. Unlike traditional polymerization, the monomer which participates in plasma polymerization does not have to have an active double bond or functional groups. Plasma polymerization of methane is a typical example of this unique polymerization. In addition, methane plasma polymer can be formed into an extremely tight network,<sup>1</sup> because of the small building unit, which not only functions as a good barrier coating but also provides excellent surface durability. Besides, it has excellent adhesion in dry and wet situations,<sup>2,3</sup> and its coating dramati-

cally reduces water vapor permeability.<sup>4</sup> Therefore, a coating of methane plasma polymer is a suitable selection for the surface modification of silicone rubber in biomedical applications.

It is known<sup>5</sup> that operating conditions, such as type of monomer, flow rate, and power supply, affect the natures of plasma and plasma polymer and are variables dependent on each other. Therefore, the composite parameter  $W/FM$  is adopted<sup>6</sup> to describe the plasma characteristics and the characteristics of the deposited film.  $W$  is the discharge power to maintain glow,  $M$  is the molecular weight of the monomer, and  $F$  is the flow rate of the monomer introduced into the system in cubic centimeters per minute (STP). Hence,  $W/FM$  is used to represent the energy supply per unit mass of the monomer. In SI units,  $W/FM$  is J/kg. Because the energy inputs required for plasma polymerization of organic compounds are in the range of  $10^8$ – $10^{11}$  J/kg, GJ/kg ( $10^9$  J/kg) is used to express  $W/FM$  in this paper. Through the relationship between deposition rate and  $W/FM$ , there are three plasma regions<sup>7</sup> divided by the composite parameter  $W/FM$ , i.e., the power-deficient region (I), the monomer-deficient region (III), and the intermediate region (II). Because the deposition rate is a function of system pressure,<sup>8</sup> this variation in relation to the three plasma regions was investigated. The correlation of the coating thickness, the surface energy, the gas permeabilities, and the elemental ratios of methane plasma coating of silicone rubber membrane are studied in relation to  $W/FM$ .

## EXPERIMENTAL

The plasma reactor system [Shimadzu Corp. (LCVD-12-400A)] is a bell jar reactor which utilizes a capacitively coupled magnetron driven by a 10-kHz audio frequency source. The reactor system consists of four main parts: a reactor chamber, a pumping unit, a gas supply unit, and a discharge power supply unit. A schematic representation of the system is shown in Figure 1.

The reactor chamber is composed of a stainless steel vacuum collar and a bell-shaped glass jar with a stainless steel outside protector, as shown in Figure 2. The jar has an outside diameter of 18.3 in., a thickness of 0.5 in., and a height of 18.8 in. A 14-in. aluminum substrate mounting plate with four 4-in. holes, positioned midway between two  $7 \times 7$  in. aluminum electrodes, is capable of rotating on an axle placed on the metal stands below the electrodes. The electrode separation was fixed at 3.4 in., and rotation was kept at 5.9 rpm.

Monomer methane gas was purchased from Matheson Co. and no further purification was used. Silicone rubber membranes were provided by a courtesy of Shin-Etsu Chemicals, Japan. The substrates were clamped at the edges of the holes in the rotating plate with brass clips during plasma polymerization. The monomer flow rate was regulated by a Tylan controller from 0.29 cm<sup>3</sup> (STP)/min to 6.6 cm<sup>3</sup> (STP)/min. The flow rate was calculated from the pressure–volume relationship by cutting off the pumping. The power supplied was varied from 25 to 188 W by adjusting current and voltage. The pressure in the reactor system was continually monitored with an MKS Baratron manometer and a Hewlett-Packard digital multimeter 3435A. In addition, using an XTM thickness monitor (Inficon Leybold-Heraeus Inc.), the deposition rate and total mass on a quartz crystal sensor were continually followed during polymerization.

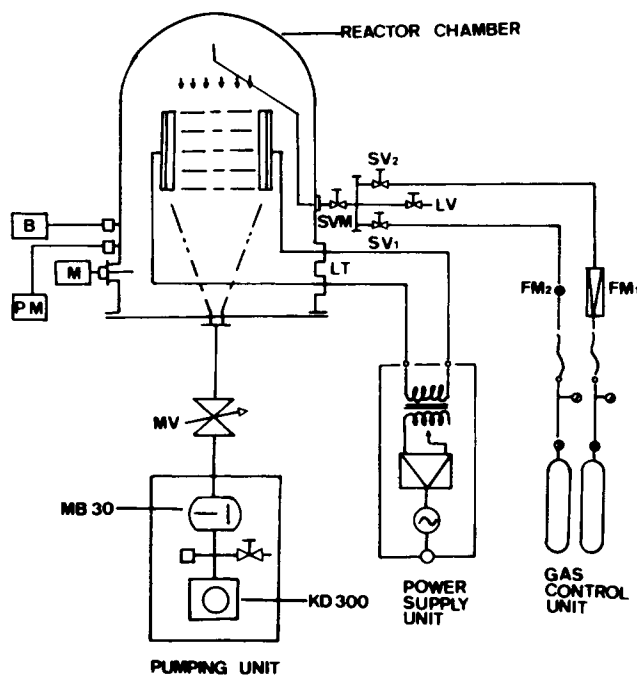


Fig. 1. Schematic presentation of plasma polymerization system.

The thickness of deposition of plasma polymer was estimated by establishing calibration factors which relate the reading of a thickness monitor (placed in a fixed position) to the thickness of deposition occurring on a rotating substrate which passes in and out of the glow discharge zone. The calibration factor was determined by depositing a plasma polymer under a set of glow discharge conditions and determining the ratio of thickness/thickness moni-

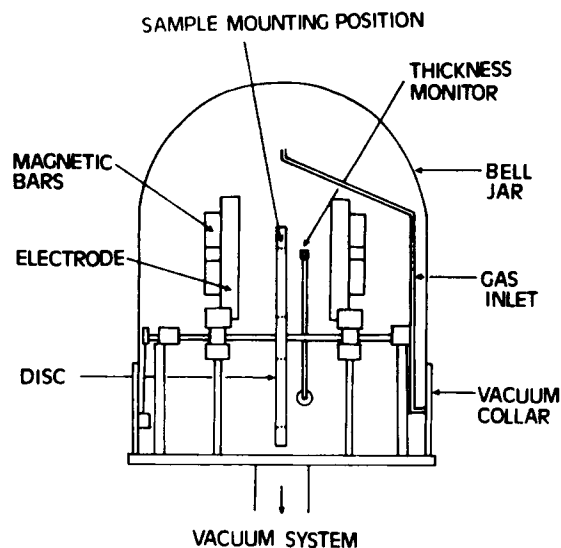


Fig. 2. Schematic presentation of plasma polymerization reactor.

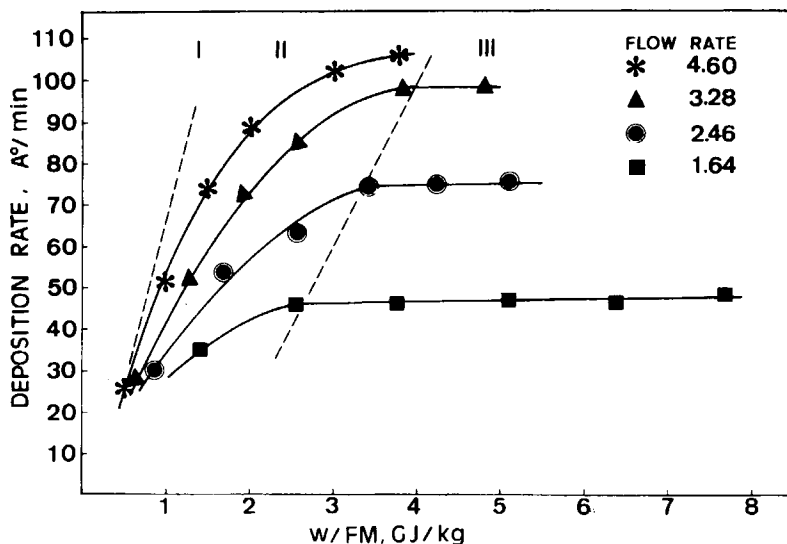


Fig. 3. Deposition rates vs.  $W/FM$  under high pumping rates (with mechanical and booster pump on).

tor reading. The thickness of the deposited polymer film on the substrate was measured by the method of interferometry.<sup>9</sup> A piece of Scotch tape was attached as a mask to a part of the microscope slide so that an abrupt step from the coated to the masked area could be found. Yellow light of 600 nm wavelength was used as the test beam.

Measurement of the contact angle was performed at room temperature using a horizontal microscope equipped with a goniometer eyepiece (Rame-Hast Inc., Mountain Lakes, NY). The surface energy and wettability of the plasma polymer coating were determined by measuring the contact angle of equilibrium sessile drops of a series of test liquids on the polymer surface. A platinum wire was used to lay the liquid drop on the solid surface.

Gas permeabilities of the methane plasma polymer coated silicone rubber membrane were measured using an isobaric gas permeability meter (GPM 200, Incentive Research and Development AB, Bromma, Sweden) described previously.<sup>10</sup> The decay method was used to measure the gas permeability of the highly permeable silicone rubber membrane.

## RESULTS AND DISCUSSION

### Deposition Rate and $W/FM$

Figure 3 depicts the dependence of the deposition rate on  $W/FM$  when the double stage pump and the mechanical booster pump are used, designated as the high pumping rate. It shows that, at any monomer flow rate, the deposition rate increases with  $W/FM$ , and beyond a critical value, the deposition rate reaches a plateau. Besides, when  $W/FM$  is over this critical point, the deposition rate increases with the flow rate at the fixed  $W/FM$ . This is because, at low  $W/FM$  for a specific flow rate, the plasma is operated in the power-deficient region with sufficient monomer, and the deposition rate

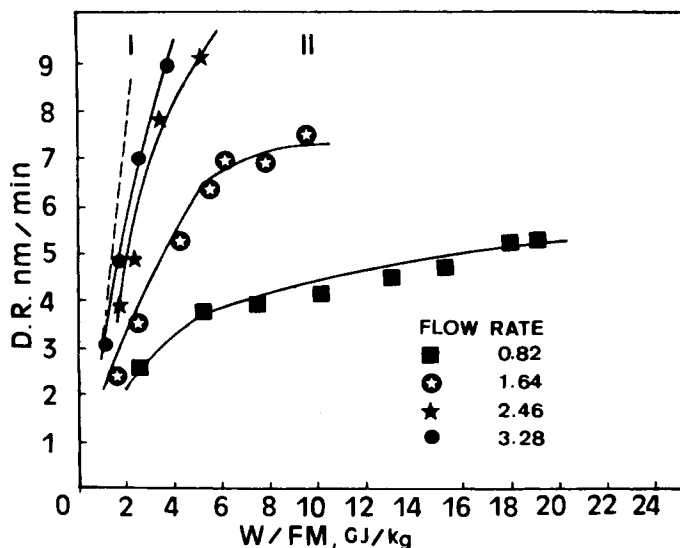


Fig. 4. Deposition rates vs.  $W/FM$  under low pumping rates (without mechanical booster pump).

is increased by the energy input parameter  $W/FM$ . When  $W/FM$  exceeds this critical point, the plasma is operated in the monomer-deficient region, and flow rate becomes the rate-determining factor. From this figure, it can be seen that, at this pumping rate, the monomer-deficient and intermediate regions are clearly seen, but the power-deficient region is not clear. Figure 4 shows the dependence of the deposition rate on  $W/FM$  when only the mechanical pump is used (low pumping rate). It illustrates that the deposition rate increases with  $W/FM$ ; then the rate of increase gradually declines as  $W/FM$  becomes higher. The power-deficient region and the intermediate region are well defined, but the monomer-deficient region cannot be obtained due to the limit of the equipment. This is because, at a lower pumping rate at a fixed flow rate, the system pressure is higher and the effective resident time of monomer for plasma polymerization increases.

In order to normalize the deposition rate without the effect of flow rate, the parameter  $DR/FM$  is introduced, in which  $DR$  represents the deposition rate of the plasma polymer. The effect of  $W/FM$  on  $DR/FM$ , the yield of plasma polymer deposition per unit mass of the monomer, for methane plasma polymerization at two kinds of pumping rates is shown in Figure 5. Despite the different power inputs and monomer flow rates, the correlation shows a single trend between the yield  $DR/FM$  and the composite factor  $W/FM$ . Comparing the relationship between  $DR/FM$  and  $W/FM$  at different pumping rates, it is interesting to note that these two curves overlap in the power-deficient region, and the values of  $DR/FM$  of high pumping rate are smaller than those of low pumping rate when  $W/FM$  is beyond the power-deficient region. Since  $DR/FM$ , which has a unit dimension of thickness/mass, is proportional to the yield of monomer to polymer deposition,<sup>11</sup>  $DR/FM$  is only a function of the polymer deposition yield  $Y_p$ , which depends on the  $W/FM$  level and the nature of the monomer. Because discharge power is the

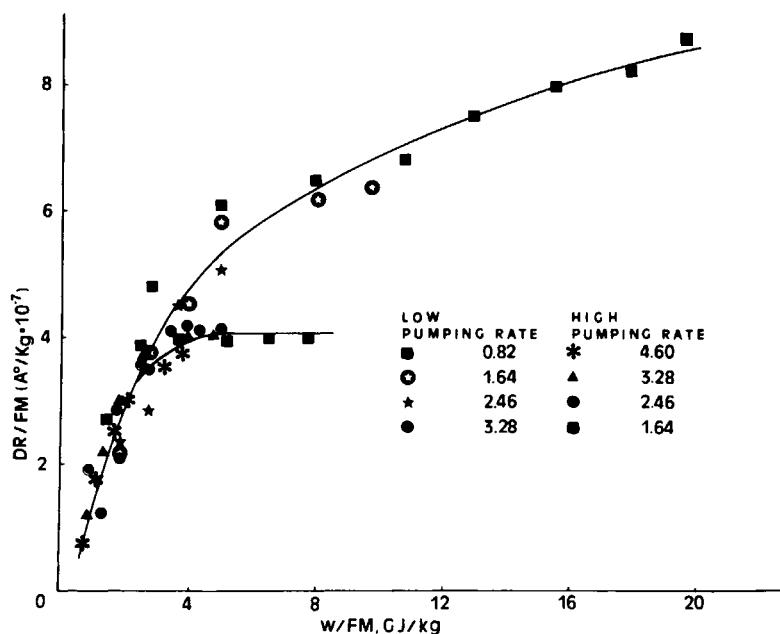


Fig. 5. Specific deposition rates vs.  $W/FM$ .

major controlling factor in the power-deficient region, the  $DR/FM$ 's of the high pumping rate and those of the low pumping rate overlap. Beyond the power-deficient region, the amount of monomer starts to play the major role. As the effective resident time of the monomers in the high pumping rate system is shorter than that in the low pumping rate system, the  $DR/FM$  of the high pumping rate system is lower than that of the low pumping rate system at the same  $W/FM$ . Besides, because more reactive species are expelled at high pumping rate, the monomer-deficient region is reached at lower  $W/FM$  in the high pumping rate system than in the low pumping rate system.

### Correlation between Real Coating Thickness and Monitor Reading Thickness

It is noted that the position and direction of the crystal sensor of the thickness monitor are not exactly the same as the position and direction of the substrate. Therefore, the reading of the monitor does not directly represent the coating thickness on the substrate. The technique of interferometry is adopted to measure the coating thickness because it has the advantage that is not necessary to take into consideration of the possible density change. The ratio  $\alpha$  of real coating thickness on the substrate to the total reading thickness of monitor vs. monomer flow rate was examined at various  $W/FM$  at low pumping rate, as shown in Figure 6. The ratio  $\alpha$  first decreased with the increase of monomer flow rate, then, after passing the critical point, it rose with flow rate. A possible explanation is as follows: When glow discharge is initiated by using a magnetron, it forms a high intensity donut-shaped ring adhering closely to the electrode surface. A less intensive glow extends beyond

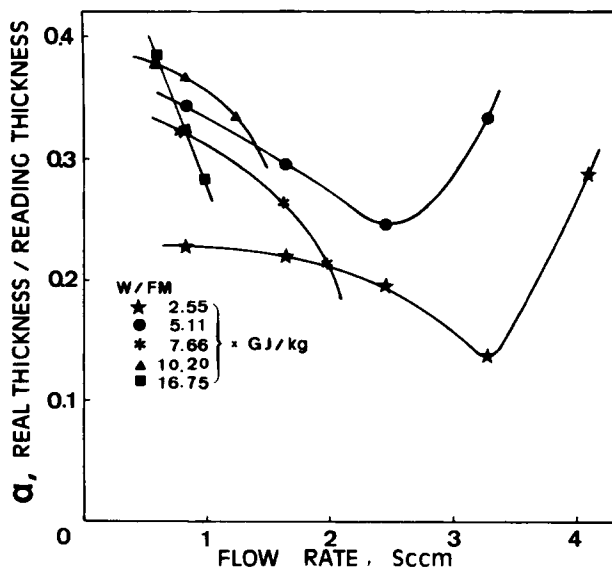


Fig. 6. Dependence of the correlation factor on flow rate and  $W/FM$ .

the intensive glow ring. As audio frequency discharge can be explained by the direct current discharge with alternating polarity, the length of the mean free path of the electrons is inversely proportional to monomer flow rate or pressure. When monomer flow rate increases, the glow shrinks and shifts toward the electrodes. Because the crystal sensor is between the rotating plate and the electrode and close to the edge of the plate, the movement of the glow results in a decrease of  $\alpha$  due to the relative shift of monitor position in the glow discharge. At constant  $W/FM$ , when the flow rate is increased, the power input increases with it. The increase of power causes the glow to expand, but the effect is not so evident as the effect of flow rate or pressure. In most conditions of the process, the power effect is less than the flow rate effect and is offset by the flow rate effect. However, when discharge power is increased to a certain large value, the power effect becomes dominant over the flow rate effect. That makes the glow expand and  $\alpha$  increase rapidly with flow rate.  $\alpha$  is used to estimate the thickness of plasma polymer layer which deposits on a silicone rubber substrate.

### Surface Energy and Wettability

Surface energy studies have been carried out for methane-plasma-polymer-coated silicone rubber membrane at various  $W/FM$  at low pumping rate. The dispersion and polar components of the surface energies of plasma polymer coating were calculated from the observed values of contact angles according to the model developed by Kaelble.<sup>12</sup> The sum of  $r_s^d$  and  $r_s^p$ , the dispersion and the polar components of the solid vapor surface free energy, should yield a reasonable approximation of the total solid surface energy,  $r_s$ . In Figure 7, total surface energy and its dispersion ( $r_s^d$ ) and polar ( $r_s^p$ ) components are plotted against  $W/FM$ . The dispersion component,  $r_s^d$ , is independent of the composite parameter  $W/FM$  in the range from 1.02 to 28.8 GJ/kg. However,



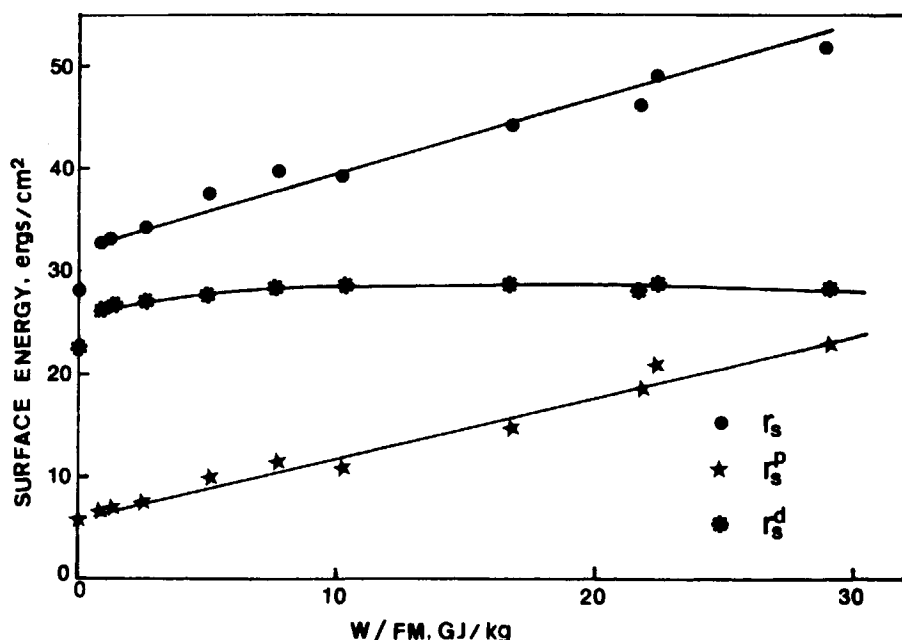


Fig. 7. Change of surface energies as functions of  $W/FM$ .

the polar contribution,  $r_s^p$ , undergoes a linear increase with  $W/FM$ . Consequently, the value of total surface energy,  $r_s$ , increases linearly with increasing  $W/FM$ . Because the dispersive and polar components of uncoated silicone rubber membrane are 22 and 6 dyn/cm, respectively, whose  $r_s$  is lower than that of methane plasma polymer coated silicone rubber membrane, the coating of methane plasma polymer significantly increases the wettability of the silicone surface.

Generally, the surface energy of plasma polymer derived from a hydrocarbon monomer is higher than that of its conventional polymer. This is due to incorporation of oxygen-containing groups onto the surface by the reaction of trapped free radicals with oxygen and/or water in the air. It is reasonable to suggest that the postplasma reaction of atmospheric oxygen and water with trapped free radicals is more likely to form hydrophilic carbonyl and hydroxyl groups<sup>13</sup> at a higher  $W/FM$ .

### Gas Permeability

Figure 8 shows the relationship between gas permeabilities of a composite film and  $W/FM$  at low pumping rate. Because silicone rubber membrane is a highly permeable material, the changes of gas permeabilities in a composite film can be used to represent the structural change of the coated plasma polymer. This figure indicates that the gas permeabilities of oxygen, nitrogen, and carbon dioxide decrease with increasing  $W/FM$ . However, after  $W/FM$  passes some specific value, they rise to around their initial values. It is known that  $W/FM$  represents the energy input per unit mass of monomer, and the higher the energy input of glow discharge is, the tighter is the network structure of the plasma polymer. Therefore, the gas permeabilities of oxygen,

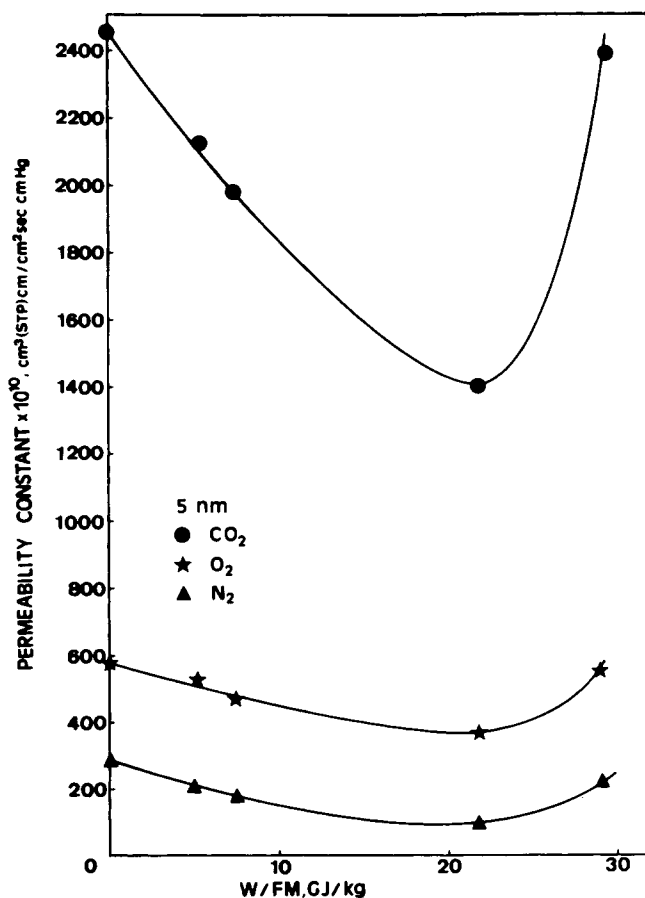


Fig. 8. Changes of permeabilities versus functions of  $W/FM$ .

nitrogen, and carbon dioxide decrease with the increase of  $W/FM$  according to the molecular sieve mechanism.<sup>4</sup> Meanwhile, a tighter structure also causes higher internal stress, which makes cracking occur more easily. When  $W/FM$  exceeds the critical value, cracks occur and gas permeabilities increase with further increase of  $W/FM$ . That is consistent with the results that the permeability constants obtained at very high  $W/FM$  are the same as those of the uncoated membrane. In a study of gas separation membranes, it was also reported<sup>14</sup> that excessive energy input would cause cracking of the film.

From comparison of Figures 8 and 4, it is suggested that film with high gas permeability is prepared in the power-deficient region, whereas, if cracking is avoided, the films prepared in the intermediate region will have low gas permeabilities. The transport characteristics of films prepared in different plasma regions are quite different.

The dependence of gas permeabilities of oxygen, nitrogen, and carbon dioxide on the coating thickness are shown in Figure 9. This figure shows that the gas permeabilities of oxygen, nitrogen, and carbon dioxide decrease with coating thickness as expected; however, after the coating thickness is over a specific value, the gas permeabilities of a composite film increase with coating

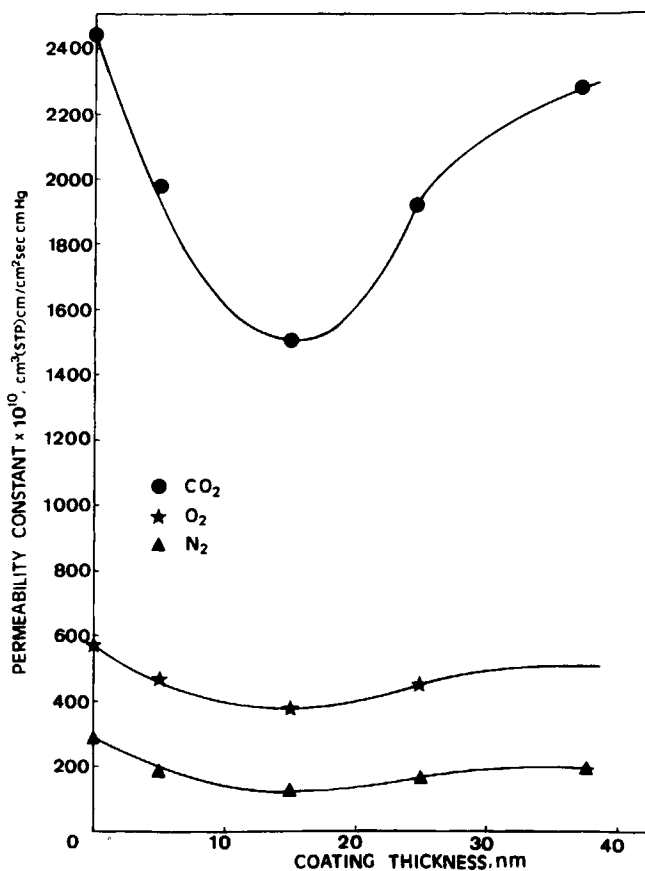


Fig. 9. Changes of permeabilities as functions of coating thickness.

thickness. It is clear that when the coating thickness increases, the resistance of the coating increases linearly with the thickness and permeabilities of a composite film decrease. On the other hand, internal stress within a coated layer increases with coating thickness, which results in cracking of the film when the coating is too thick.

Selectivity is related to the solubilities of permeant molecules in the membrane and also depends on whether the free volume between the polymer chains is small and restricted enough to distinguish different-size permeant molecules. The permselectivities of the CO<sub>2</sub>, O<sub>2</sub> pair, CO<sub>2</sub>, N<sub>2</sub> pair, and N<sub>2</sub>, O<sub>2</sub> pair were investigated at different  $W/FM$ , as shown in Figure 10. The permselectivities of the CO<sub>2</sub>, O<sub>2</sub> pair, and the O<sub>2</sub>, N<sub>2</sub> pair are almost independent of  $W/FM$ , while the selectivity ratio of CO<sub>2</sub> and N<sub>2</sub> varies between 8 and 14. The results indicate that the solution-diffusion mechanism is predominant due to the higher permeability of the CO<sub>2</sub> molecule as compared to that of the N<sub>2</sub> molecule, resulting from the higher solubility of CO<sub>2</sub> in the membrane. Therefore, it is concluded that the permeability characteristics of the plasma polymer of methane fall between the solution-diffusion mechanism and the molecular sieve mechanism.

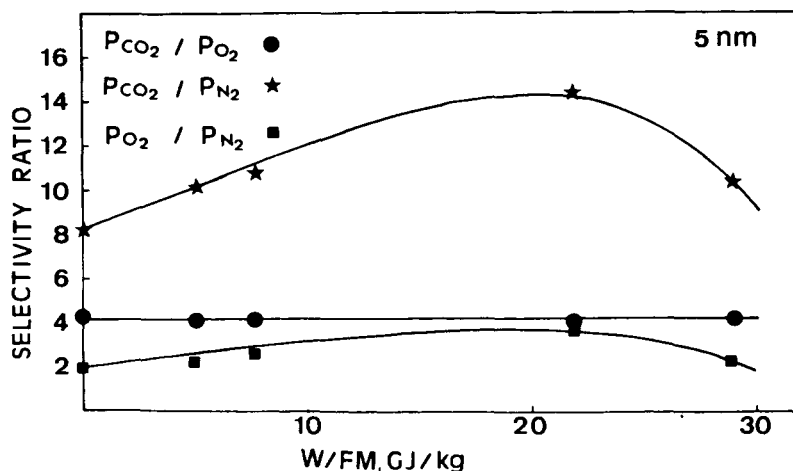


Fig. 10. Changes of selectivity ratios as functions of  $W/FM$ .

### ESCA

The relationship between the elemental ratios, O/C and Si/C from ESCA, with  $W/FM$  at the low pumping rate, is shown in Figure 11. The ratio O/C increases with the increase of  $W/FM$ , which is consistent with the increase in polar surface energy with  $W/FM$ , as shown in Figure 7. It is generally observed that plasma polymer of hydrocarbon deposited on a silicone rubber substrate nearly always shows a small amount of Si ESCA signal even when the thickness of deposition exceeds the electron escaping depth. This phenomenon has been attributed to the high volatility of silicon-containing materials in plasma.<sup>15</sup> The elemental ratio of Si/C generally increases with increasing  $W/FM$ .<sup>16</sup> It is suggested that the nature of the substrate indeed affects the characteristics of the coating.

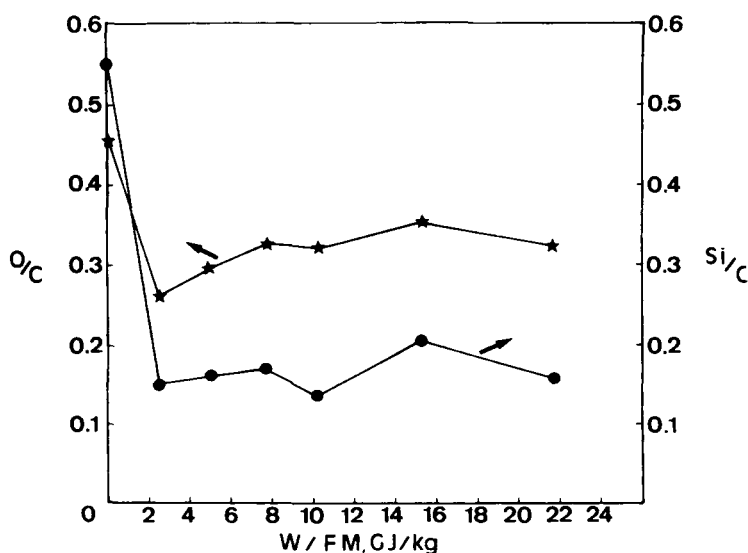


Fig. 11. Elemental ratio O/C and Si/C by ESCA as functions of  $W/FM$ .

## CONCLUSIONS

Because  $DR/FM$  is only a function of the total deposition yield,  $Y_p$ , which depends on the  $W/FM$  level and the discharge power, is the major controlling factor in the power-deficient region. The  $DR/FM$  is not affected by the pumping rate in this region. When the composite parameter  $W/FM$  is beyond the power-deficient region, the amount of the monomer plays the major role. Due to the increase of the effective resident time, the  $DR/FM$  in the low pumping rate system is larger than that in the high pumping rate system; in other words, the deposition is more efficient in the low pumping rate system.

Due to the fully developed crosslinked structure of methane plasma polymer, the dispersion component of surface energy is independent of the composite parameter  $W/FM$ . However, the polar component undergoes a linear increase with  $W/FM$ ; the reason is that the oxygen-containing groups incorporate onto the surface, which is supported by the ESCA results.

The effect of coating thickness of methane plasma polymer on the gas permeability of the silicone rubber membrane is remarkable. Gas permeabilities change with coating thickness due to the integrity and the internal stress of the methane plasma coating.

The results also suggest that the transport characteristics of the silicone composite films coated with methane plasma polymer in different plasma regions are different. Namely, film with high gas permeability is prepared in the power-deficient region; and, if cracking is avoided, composite films prepared in the intermediate region show low gas permeabilities.

## References

1. H. Yasuda, Ashok K. Sharma, and Takeshi Yasuda, *J. Polym. Sci. Polym. Phys. Ed.*, **19**, 1285 (1981).
2. N. Inagaki and H. Yasuda, *J. Appl. Polym. Sci.*, **26**, 3333 (1981).
3. K. C. Mittal, *Adhesion Aspects of Polymeric Coatings*, Plenum, New York, 1983.
4. H. Yasuda, *Plasma Polymerization*, Academic, New York, 1985, Chap. 10.
5. H. Yasuda, *J. Polym. Sci. Macrom. Rev.*, **16**, 199 (1981).
6. H. Yasuda and T. Hirotsu, *J. Polym. Sci. Polym. Chem. Ed.*, **16**, 743 (1978).
7. H. Yasuda and C. R. Wang, *J. Polym. Sci. Polym. Chem. Ed.*, **23**, 87 (1985).
8. N. Morosoff, W. Newton, and H. Yasuda, *J. Vac. Sci. Technol.*, **15**(6), 1815 (1978).
9. A. Piegari and E. Masetti, *Thin Solid Films*, **124**, 249 (1985).
10. H. Yasuda and K. J. Rosengren, *J. Appl. Polym. Sci.*, **14**, 2839 (1970).
11. Y. S. Yeh, I. N. Shyy, and H. Yasuda, *Appl. Polym. Sym.*, **42**, 1 (1988).
12. D. H. Kaelble, *Physical Chemistry of Adhesion*, Wiley, New York, 1971.
13. H. Yasuda, H. C. Marsh, S. Brandt, and C. N. Reilley, *J. Polym. Sci. Polym. Chem. Ed.*, **15**, 991 (1977).
14. H. Nomura, P. W. Kramer, and H. Yasuda, *Thin Solid Films*, **118**, 187 (1985).
15. Y. S. Yeh and H. Yasuda, *J. Polym. Sci. Polym. Chem. Ed.*, **24**, 3233 (1986).
16. C. L. Hamermesh and P. J. Dynes, *J. Polym. Sci. Polym. Lett. Ed.*, **13**, 663 (1975).

Received June 26, 1989

Accepted July 10, 1989